Hydrothermal Syntheses and Crystal Structures of Two New Iron Phosphates $[C_2N_2H_{10}]^{2+}[Fe(HPO_4)_2(OH)]^{2-} \cdot H_2O$ and $KFe_3(OH)_2(PO_4)_2 \cdot 2H_2O$

Zoe A. D. Lethbridge, Philip Lightfoot,[1] Russell E. Morris, David S. Wragg, and Paul A. Wright

School of Chemistry, University of St. Andrews, St. Andrews, Fife, KY16 9ST, UK

and

Åke Kvick and Gavin Vaughan

ESRF, BP220 38043 Grenoble Cedex, France

 Two new iron phosphates have been prepared hydrothermally and characterized by single crystal X-ray diffraction. $[C_2N_2H_{10}]^{2+}[Fe(HPO_4)_2(OH)]^{2-} \cdot H_2O$ (I) crystallizes in triclinic space group *P*-1, $a = 8.526(2)$ Å, $b = 9.796(2)$ Å, $c = 7.232(2)$ Å, $\alpha = 90.25(2)°$, $\beta = 92.72(2)°$, $\gamma = 65.20(1)°$, $Z = 2$, R, $R_w = 0.040, 0.044$. The structure is composed of isolated anionic chains of the tancoite type, $[Fe(HPO_4)_2OH]_n$, consisting of vertex-sharing Fe–O octahedra. The chains are isotypic with those in the iron fluorophosphate ULM-14, but in that case the vertex-sharing is via an F^- link rather than an OH^- link. $KFe_3(OH)_2(PO_4)_2 \cdot 2H_2O$ (II) adopts the orthorhombic space group $Pmc2_1$, $a = 6.410(2)$ Å, $b = 7.429(3)$ Å, $c = 9.868(4)$ Å, $Z = 2$, R, $R_w = 0.053, 0.090$. In this case the structure was solved from microcrystal diffraction data at a synchrotron source (crystal size $60 \times 15 \times 5$ µm). The structure is isotypic with the mineral olmsteadite, $KFe_2NbO_2(PO_4)_2 \cdot 2H_2O$, with Fe^{3+} on the Nb^{5+} site and charge-balancing OH^- groups replacing O^{2-}. This compound has a three-dimensional framework structure with small channels running parallel to *a* and *c* in which the K^+ ions sit. © 1999 Academic Press

INTRODUCTION

Despite the existence of many naturally occuring iron phosphate minerals exhibiting a rich and varied structural chemistry (1), the synthetic hydrothermal chemistry of iron phosphates has only recently gained popularity, driven largely by the quest for preparing new open-framework materials with potentially interesting sorptive, catalytic, or magnetic properties. Examples of materials which have been

prepared in this way include one-dimensional (2), two-dimensional (3–5), and three-dimensional (6–9) structures. The variable oxidation state and coordination preferences of iron mean that the structural chemistry of these materials is complex, and the field promises a wider range of materials than occurs, for example, in aluminosilicate or aluminophosphate chemistry. Recently, we have begun an exploratory study of hydrothermal systems involving mixed organic–inorganic anion components, where the inorganic anion is PO_4^{3-} and the organic anion is a multidentate carboxylic acid, for example oxalate. Our first success in preparing a mixed framework structure of this type has recently been reported, viz. $Fe_4(PO_4)_2(C_2O_4) \cdot 2H_2O$ (10). This paper describes the results of two further reactions in $Fe–PO_4–C_2O_4$ systems, which have produced two new iron phosphates, both of which are related to known mineral structure types.

EXPERIMENTAL

$[C_2N_2H_{10}]^{2+}[Fe(HPO_4)_2(OH)]^{2-} \cdot H_2O$ (compound **I**) was prepared by hydrothermal reaction of $Fe(C_2O_4) \cdot 2H_2O$, H_3PO_4 (85%), and $NH_2(CH_2)_2NH_2$ in water in a molar ratio of 1:1:1:200. The reactants were heated in a Teflon-lined steel autoclave for 39 h at 160°C. The product was filtered, washed with distilled water, and dried in air. The product consisted of a predominant phase of yellow powder, identified by X-ray powder diffraction as $Fe(C_2O_4) \cdot 2H_2O$, together with a small amount of brown crystalline material (subsequently characterized as **I**). Crystal structure analysis was carried out on a Rigaku AFC7S automated four-circle diffractometer, equipped with Mo$K\alpha$ radiation. Details of the data collection and analysis are

[1]To whom correspondence should be addressed. Fax: 44-1334-463808. E-mail: pl@st-and.ac.uk.

TABLE 1
Crystal Data and Details of Structure Solution and Refinement

	I	II
Formula	$[C_2N_2H_{10}]^{2+}[Fe(HPO_4)_2(OH)]^{2-} \cdot H_2O$	$KFe_3(OH)_2(PO_4)_2 \cdot 2H_2O$
Crystal system	Triclinic	Orthorhombic
Space group	P-1	$Pmc2_1$
Cell parameters	$a = 8.526(2)$ Å	$a = 6.410(2)$ Å
	$b = 9.796(2)$ Å	$b = 7.429(3)$ Å
	$c = 7.232(2)$ Å	$c = 9.868(4)$ Å
	$\alpha = 90.25(2)$	
	$\beta = 92.72(2)°$	
	$\gamma = 65.20(1)°$	
Crystal colour	Brown	Brown
Crystal dimensions (mm)	0.50, 0.30, 0.02	0.060, 0.015, 0.005
Z	2	2
ρ_{calc} (g cm^{-3})	2.09	3.26
2θ (max)°	50.0	50.3
Total unique reflections	1522	2034
Observed reflections ($I > 3\sigma(I)$)	1268	3431
No. of variables	202	96
R, R_w	0.040, 0.044	0.053, 0.090

given in Table 1. The structure was solved using heavy atom methods (11) and expanded using Fourier techniques. All subsequent refinement was carried out using the teXsan package (12). All nonhydrogen atoms were refined anisotropically. Bond valence sum analysis (13) was used to deduce the oxidation states of the two crystallographically independent iron atoms (3.08 and 3.02 v.u. for Fe(1) and Fe(2) respectively, hence unambiguously assigning both as Fe^{3+}), and also to infer the locations of hydrogen atoms (1.10, 1.06, and 1.14 v.u. for O(1), O(6), and O(9), respectively, hence assigning these as OH^- groups). Charge balance suggests that the ethylenediamine is doubly protonated. All hydrogen atoms, including those on the water molecule O(10), were subsequently found from difference Fourier data and refined isotropically.

KFe$_3$(OH)$_2$(PO$_4$)$_2 \cdot$ 2H$_2$O (**II**) was prepared by hydrothermal reaction of Fe(C$_2$O$_4$) $\cdot$ 2H$_2$O and K$_3$PO$_4 \cdot$ H$_2$O in water in a molar ratio of 1:1:200, at 160°C for 18 h. The product consisted of a predominant phase of brown crystals, together with a dark green polycrystalline material. The major phase was subsequently characterized as compound **II**; the minor phase could not be identified. The crystals were too small to analyze on the AFC7S, so structure determination was carried out at the ID-11 beam-line at the ESRF, Grenoble. The microcrystal was glued to the end of a fine glass fibre and data collected on a three-circle (fixed kappa) Siemens diffractometer fitted with a Siemens SMART CCD detector, at room temperature. The wavelength was calibrated prior to the experiment as 0.4425 Å. Data were collected in ω intervals of 0.1° over 140°, with the detector covering a fixed 2θ range. The resolution limit was

0.502 Å. Data reduction was carried out using the Siemens SAINT software adapted for synchrotron use and further data analysis carried out using the DIRDIF (11) and teXsan (12) suites. Systematic absences were consistent with space groups $Pmcm$, $P2cm$, or $Pmc2_1$. As no solution could be obtained in the former cases, the latter was assumed. This is

TABLE 2
Final Atomic Coordinates and Equivalent Isotropic Temperature Factors for I, Space Group P-1, $a = 8.526(2)$ Å, $b = 9.796(2)$ Å, $c = 7.232(2)$ Å, $\alpha = 90.25(2)°$, $\beta = 92.72(2)°$, $\gamma = 65.20(1)°$

Atom	x	y	z	B (eq)
Fe(1)	1.0000	0.0000	0.5000	0.84(3)
Fe(2)	1.0000	0.0000	0.0000	0.84(3)
P(1)	1.0182(2)	0.2724(2)	0.2654(2)	1.14(4)
P(2)	0.6444(2)	0.1746(2)	0.2284(2)	1.02(4)
O(1)	1.0633(5)	−0.0889(5)	0.2515(5)	0.91(9)
O(2)	1.0711(5)	0.1666(4)	0.4341(5)	1.16(10)
O(3)	0.7560(5)	0.1212(5)	0.4063(5)	1.42(9)
O(4)	1.0234(5)	0.1865(5)	0.0873(5)	1.28(9)
O(5)	0.8503(5)	0.4068(5)	0.2882(6)	1.8(1)
O(6)	1.1526(6)	0.3449(5)	0.2540(7)	1.6(1)
O(7)	0.7448(5)	0.0956(5)	0.0599(5)	1.22(9)
O(8)	0.4794(5)	0.1529(5)	0.2388(6)	1.6(1)
O(9)	0.5853(6)	0.3482(5)	0.2055(6)	1.9(1)
O(10)	0.7177(8)	0.3873(6)	0.6766(9)	4.2(2)
N(1)	0.5719(7)	0.1032(7)	0.7172(8)	1.7(1)
N(2)	0.1007(7)	0.3227(7)	0.7658(8)	1.7(1)
C(1)	0.2847(9)	0.2430(9)	0.8307(9)	1.9(2)
C(2)	0.4009(9)	0.2264(9)	0.6749(10)	2.0(2)

Note. Hydrogen atoms not included.

TABLE 3
Selected Bond Distances and Angles for I

Fe(1)	O(1)	1.988(4)	×2		P(1)	O(2)	1.530(4)	
Fe(1)	O(2)	2.029(4)	×2		P(1)	O(4)	1.527(4)	
Fe(1)	O(3)	2.005(4)	×2		P(1)	O(5)	1.499(4)	
Fe(2)	O(1)	1.975(4)	×2		P(1)	O(6)	1.586(5)	
Fe(2)	O(4)	2.016(4)	×2		P(2)	O(3)	1.525(4)	
Fe(2)	O(7)	2.040(4)	×2		P(2)	O(7)	1.528(4)	
					P(2)	O(8)	1.513(4)	
					P(2)	O(9)	1.565(5)	
C(1)	C(2)	1.49(1)						
N(1)	C(2)	1.472(9)						
N(2)	C(1)	1.487(9)						

O(1)	Fe(1)	O(1)	180.00		O(1)	Fe(2)	O(1)	180.00	
O(1)	Fe(1)	O(2)	90.4(2)	×2	O(1)	Fe(2)	O(4)	90.5(2)	×2
O(1)	Fe(1)	O(2)	89.6(2)	×2	O(1)	Fe(2)	O(4)	89.5(2)	×2
O(1)	Fe(1)	O(3)	90.5(2)	×2	O(1)	Fe(2)	O(7)	90.8(2)	×2
O(1)	Fe(1)	O(3)	89.5(2)	×2	O(1)	Fe(2)	O(7)	89.2(2)	×2
O(2)	Fe(1)	O(2)	180.00		O(4)	Fe(2)	O(7)	90.1(2)	×2
O(2)	Fe(1)	O(3)	92.0(2)	×2	O(4)	Fe(2)	O(7)	89.9(2)	×2
O(2)	Fe(1)	O(3)	88.0(2)	×2	O(4)	Fe(2)	O(4)	180.00	
O(3)	Fe(1)	O(3)	180.00		O(7)	Fe(2)	O(7)	180.00	

O(2)	P(1)	O(4)	111.0(2)		O(3)	P(2)	O(7)	111.2(2)
O(2)	P(1)	O(5)	112.5(2)		O(3)	P(2)	O(8)	111.2(2)
O(2)	P(1)	O(6)	107.8(3)		O(3)	P(2)	O(9)	108.9(3)
O(4)	P(1)	O(5)	113.7(2)		O(7)	P(2)	O(8)	110.9(2)
O(4)	P(1)	O(6)	108.5(2)		O(7)	P(2)	O(9)	109.1(3)
O(5)	P(1)	O(6)	102.8(2)		O(8)	P(2)	O(9)	105.5(3)

Fe(1)	O(1)	Fe(2)	131.8(2)		N(2)	C(1)	C(2)	110.3(6)
Fe(1)	O(2)	P(1)	129.8(2)		N(1)	C(2)	C(1)	109.7(6)
Fe(1)	O(3)	P(2)	142.3(2)					
Fe(2)	O(4)	P(1)	139.9(3)					
Fe(2)	O(7)	P(2)	134.6(2)					

Hydrogen bonds

A	H	B	A–H	H…B	A…B	A–H…B
O(1)	H(13)	O(10)	0.73(6)	2.04(6)	2.768(7)	177(7)
O(6)	H(15)	O(8)	0.70(7)	1.95(7)	2.634(6)	166(8)
O(9)	H(14)	O(5)	0.82(7)	1.79(7)	2.600(7)	169(7)
O(10)	H(11)	O(9)	1.18(6)	2.85(6)	2.942(7)	159(4)
N(1)	H(5)	O(8)	1.05(7)	1.69(7)	2.743(8)	175(5)
N(1)	H(6)	O(7)	0.88(7)	1.96(7)	2.818(7)	164(6)
N(1)	H(7)	O(3)	0.95(7)	1.91(7)	2.840(7)	165(6)
N(2)	H(8)	O(2)	0.91(6)	1.99(7)	2.898(7)	179(6)
N(2)	H(9)	O(5)	0.88(7)	2.06(7)	2.881(7)	154(6)
N(2)	H(10)	O(4)	1.09(6)	1.97(6)	2.916(7)	143(5)

the standard setting of the space group $Pb2_1m$ reported for olmsteadite (14), $KFe_2(Nb,Ta)O_2(PO_4)_2 \cdot 2H_2O$, to which the unit cell data suggested that phase **II** would be closely related. All nonhydrogen atoms were successfully located and refined anisotropically. Bond valence sum analysis suggested an ordered distribution of Fe^{2+} (Fe(1)–2.34 v.u.) and Fe^{3+} (Fe(2)–3.13 v.u.) and the assignment of O(1) as a water molecule (0.48 v.u.) and O(5) and O(6) as OH^- groups, bridging Fe(1)–O(H)–Fe(2) (0.80 and 1.18 v.u. for O(5) and

TABLE 4
Final Atomic Coordinates and Equivalent Isotropic Temperature Factors for II, Space Group $Pmc2_1$, $a = 6.410(2)$ Å, $b = 7.429(3)$ Å, $c = 9.868(4)$ Å

Atom	x	y	z	B (eq)
Fe(1)	0.2356(1)	0.0305(1)	0.0046	0.63(1)
Fe(2)	0.0000	−0.2876(2)	−0.2385(2)	0.27(2)
K(1)	0.5000	0.4679(4)	0.5341(3)	1.97(5)
P(1)	0.5000	−0.1860(2)	−0.2362(3)	0.26(3)
P(2)	0.0000	−0.3236(3)	0.0860(2)	0.45(3)
O(1)	0.2684(8)	0.2731(7)	−0.1114(6)	1.39(9)
O(2)	0.5000	0.0870(10)	0.1267(8)	1.3(1)
O(3)	0.5000	−0.0506(10)	−0.1190(7)	1.1(1)
O(4)	0.1984(6)	−0.2052(6)	0.1025(5)	0.83(7)
O(5)	0.0000	−0.0475(9)	−0.1304(7)	0.9(1)
O(6)	0.0000	0.1526(9)	0.0976(7)	1.1(1)
O(7)	0.3097(6)	−0.3069(6)	−0.2277(6)	1.05(8)
O(8)	0.0000	−0.4215(8)	−0.0523(6)	0.65(10)
O(9)	0.0000	−0.4602(9)	0.1984(6)	1.0(1)

Note. Hydrogen atoms not included.

O(6), respectively). It was not possible to locate the H atoms directly in this structure.

Final refined atomic parameters for **I** and **II** are given in Tables 2 and 4 and selected bond lengths and angles in Tables 3 and 5, respectively.
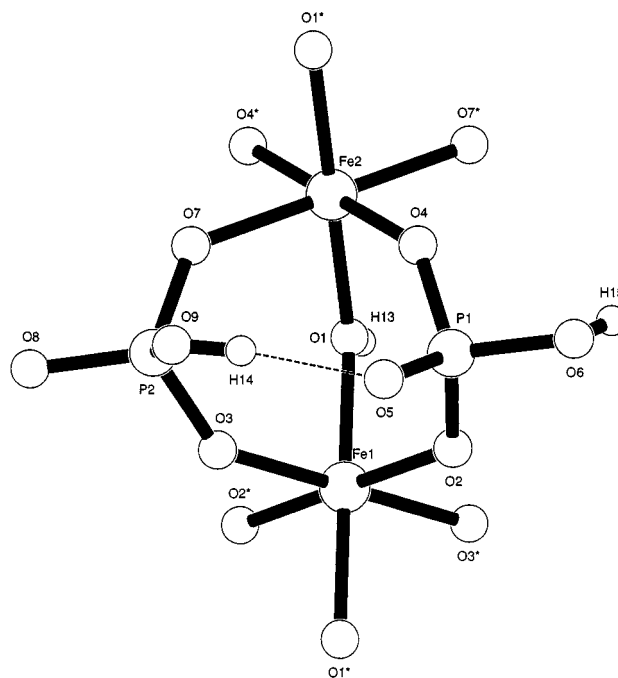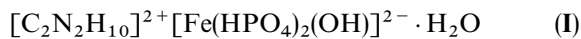

FIG. 1. Atom labeling scheme for **I**, showing the two FeO_6 octahedra and two PO_4 tetrahedra.

TABLE 5
Selected Bonds Distances and Angles for II

Fe(1)	O(1)	2.146(5)			Fe(2)	O(8)	2.090(6)	
Fe(1)	O(2)	2.121(4)			Fe(2)	O(9)	1.975(7)	
Fe(1)	O(3)	2.173(4)			P(1)	O(2)	1.541(7)	
Fe(1)	O(4)	2.014(5)			P(1)	O(3)	1.532(7)	
Fe(1)	O(5)	2.096(5)			P(1)	O(7)	1.518(4)	×2
Fe(1)	O(6)	1.987(4)			P(2)	O(4)	1.555(4)	×2
Fe(2)	O(5)	2.078(6)			P(2)	O(8)	1.547(6)	
Fe(2)	O(6)	1.902(7)			P(2)	O(9)	1.502(7)	
Fe(2)	O(7)	1.993(4)	×2					
K(1)	O(1)	2.822(6)	×2					
K(1)	O(4)	2.829(5)	×2					
K(1)	O(7)	3.097(6)	×2					
K(1)	O(7)	3.132(6)	×2					

H-bonding contacts

O(1)	O(4)	2.903(7)
O(1)	O(8)	2.906(8)
O(6)	O(7)	2.868(7)

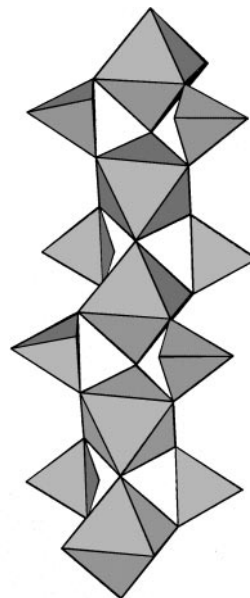| O(1)	Fe(1)	O(2)	93.3(2)		O(5)	Fe(2)	O(6)	89.1(3)	
O(1)	Fe(1)	O(3)	81.8(3)		O(5)	Fe(2)	O(7)	92.0(2)	×2
O(1)	Fe(1)	O(4)	176.3(2)		O(5)	Fe(2)	O(8)	87.5(3)	
O(1)	Fe(1)	O(5)	87.9(2)		O(5)	Fe(2)	O(9)	167.5(3)	
O(1)	Fe(1)	O(6)	86.4(3)		O(6)	Fe(2)	O(7)	94.8(2)	×2
O(2)	Fe(1)	O(3)	75.6(2)		O(6)	Fe(2)	O(8)	176.6(3)	
O(2)	Fe(1)	O(4)	89.7(2)		O(6)	Fe(2)	O(9)	103.4(3)	
O(2)	Fe(1)	O(5)	172.5(2)		O(7)	Fe(2)	O(7)	169.7(3)	
O(2)	Fe(1)	O(6)	104.8(2)		O(7)	Fe(2)	O(8)	85.3(2)	
O(3)	Fe(1)	O(4)	96.9(2)		O(7)	Fe(2)	O(9)	87.0(1)	×2
O(3)	Fe(1)	O(5)	97.4(2)		O(7)	Fe(2)	O(8)	85.3(2)	
O(3)	Fe(1)	O(6)	168.1(3)		O(8)	Fe(2)	O(9)	79.9(2)	
O(4)	Fe(1)	O(5)	88.8(2)						
O(4)	Fe(1)	O(6)	94.9(2)		Fe(1)	O(2)	Fe(1)	106.1(3)	
O(5)	Fe(1)	O(6)	82.7(2)		Fe(1)	O(2)	P(1)	126.4(1)	×2
					Fe(1)	O(3)	Fe(1)	102.5(3)	
O(2)	P(1)	O(3)	110.5(4)		Fe(1)	O(3)	P(1)	127.3(2)	×2
O(2)	P(1)	O(7)	109.3(3)	×2	Fe(1)	O(4)	P(2)	122.6(2)	
O(3)	P(1)	O(7)	110.3(3)	×2	Fe(1)	O(5)	Fe(1)	92.2(3)	
O(7)	P(1)	O(7)	107.0(3)		Fe(1)	O(5)	Fe(2)	124.3(2)	×2
					Fe(1)	O(6)	Fe(1)	99.0(3)	
O(4)	P(2)	O(4)	109.8(4)		Fe(1)	O(6)	Fe(2)	129.3(2)	×2
O(4)	P(2)	O(8)	111.0(2)	×2	Fe(2)	O(7)	P(1)	139.0(3)	
O(4)	P(2)	O(9)	107.8(2)	×2	Fe(2)	O(8)	P(2)	123.5(4)	
O(8)	P(2)	O(9)	109.5(3)		Fe(2)	O(9)	P(2)	150.8(4)	

FIG. 2. Polyhedral representation of a section of the $[Fe(HPO_4)_2OH]_n$ chain in **I**.

unit. The four remaining vertices of each octahedron are linked to four different HPO_4 groups, with each HPO_4 group in turn bridging adjacent Fe(1)–Fe(2) pairs. The basic building unit is shown in Fig. 1, and the polyhedral chain arrangement is shown in Fig. 2. The noncoordinating oxygen atoms of the HPO_4 groups participate in intra- and interchain H-bonding (see Table 3). All the protons of the ethylenediammonium cation also act as H-bond donors. A projection of the structure down the chain axis, showing the layout of adjacent chains and template/water molecules, is given in Fig. 3.

The $[M(TO_4)_2L]_n$ chain (M = an octahedral metal, T = a tetrahedral element, L = an anionic ligand, e.g., O^{2-}, OH^-, or F^-) present in this structure is a common theme in

RESULTS AND DISCUSSION

$$[C_2N_2H_{10}]^{2+}[Fe(HPO_4)_2(OH)]^{2-} \cdot H_2O \qquad \text{(I)}$$

The structure of **I** consists of anionic chains of stoichiometry $[Fe(HPO_4)_2OH]_n$ parallel to the c-axis, with templating diammonium cations and water molecules between the chains and held in via H-bonding. The core of each chain is a trans-edge-shared arrangement of alternating Fe(1)O_6 and Fe(2)O_6 octahedra, with the shared apex being the O(1)H^-
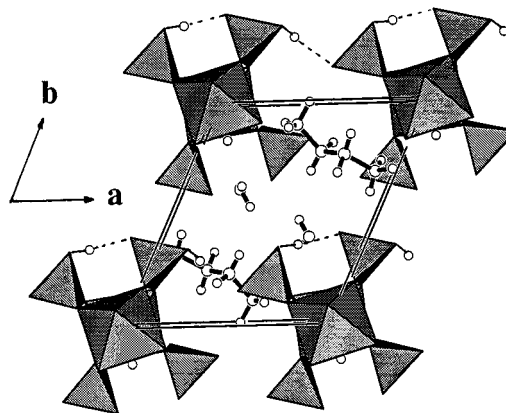

FIG. 3. Projection of the structure of **I** down the c-axis, showing water and ethylenediammonium moeities.

many mineralogical structures related to tancoite, as re-
viewed by Hawthorne (15) and also in several recently
synthesized materials. In particular the direct analog of this
chain with F^- replacing OH^- has been observed in the
synthetic materials ULM-15 (8) and ULM-14 (2), and an
aluminophosphate variant with an OH^- bridging unit has
been prepared by Attfield et al. (16).

$$KFe_3(OH)_2(PO_4)_2 \cdot 2H_2O \qquad \textbf{(II)}$$

The structure of **II** may be described as a synthetic rela-
tive of the mineral Olmsteadite (14), $KFe_2(Nb,Ta)O_2$
$(PO_4)_2 \cdot 2H_2O$. In the present structure the Nb^{5+} site is
filled by Fe^{3+}, and charge-compensation is provided by
replacing the oxide by hydroxide units. Hence, our material
is a mixed valence iron phosphate with ordering of
Fe^{2+}/Fe^{3+} on two distinct crystallographic sites. The struc-
ture has a three-dimensional array of linked FeO_6
octahedra and PO_4 tetrahedra enclosing cavities, within
which the large K^+ ions reside. However, it may be instruc-
tive to discuss the framework in terms of simpler building
units. The basic unit is shown in Fig. 4, which consists of
a vertex-linked core of FeO_6 and PO_4 polyhedra very
similar to that in **I**. However, the nature of the linkage
between these units leads to an entirely different structure to
that of **I**. The dominant feature of the structure is the chain
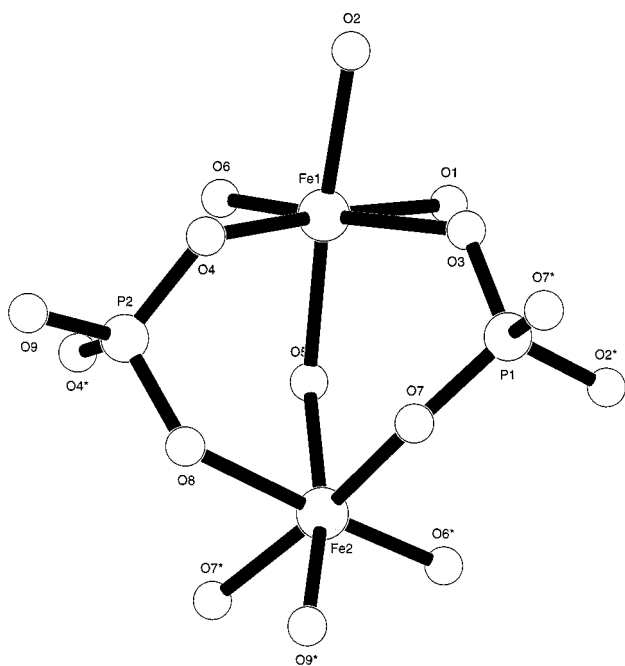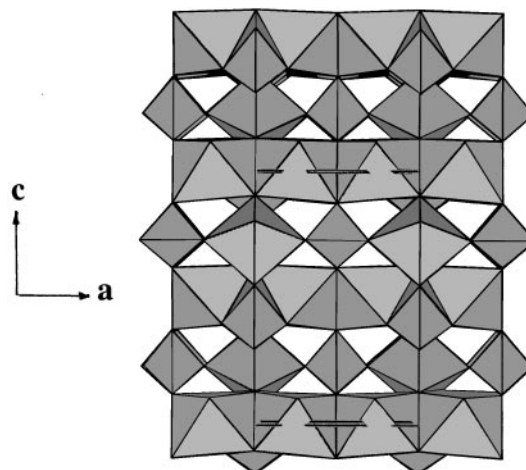of edge-shared $Fe(1)^{2+}O_6$ octahedra running parallel to the

FIG. 5. A layer in the structure of **II** projected down the b-axis,
showing edge-linked chains of $Fe(1)O_6$ octahedra linked by vertex-linked
chains of $P(1)O_4$ and $Fe(2)O_6$ polyhedra.

a-axis (Fig. 5). The edge-sharing occurs via hydroxyl groups
at O(5) and O(6). Of the remaining vertices of the $Fe(1)O_6$
octahedron, three are shared with PO_4 groups, while the
last, O(1), is a water molecule. The edge-sharing chains are
linked into sheets in the ac plane via a parallel chain of
vertex-shared $Fe(2)O_6$ and $P(1)O_4$ polyhedra which link to
the $Fe(1)O_6$ octahedra via O(5)/O(6) and O(2)/O(3), respec-
tively. Intrachain linkage in this chain occurs exclusively via
O(7). The layers are joined together in the b direction by
$P(2)O_4$ tetrahedra, which "cap" neighboring Fe(1) within
the chains, and link across the layers to Fe(2) via O(8) and
O(9) (Fig. 6). This creates a small channel in the c direction
for the K^+ cation. Small "butterfly" shaped channels may
also be seen in the a direction (Fig. 7), which also shows the

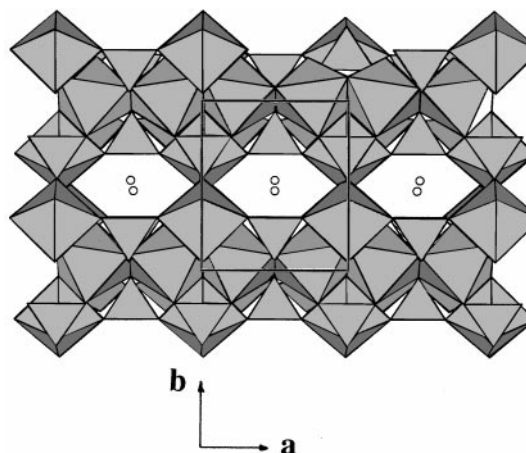**FIG. 4.** Atom labeling scheme for **II**.

FIG. 6. Projection of the structure of **II** along the c-axis, showing
linking of adjacent layers by P(2) and Fe(2). K^+ ions are shown as small
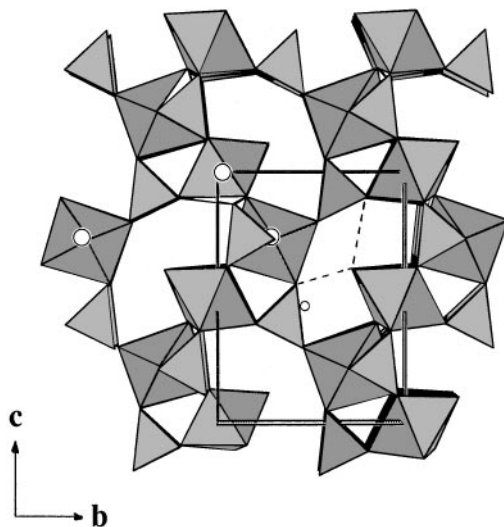spheres within the channels.

FIG. 7. Projection of the structure of **II** along the *a*-axis, showing cross-channel H-bonding.

nature of H-bonding from the water molecule O(1) (see also Table 5). Hawthorne (15) described olmsteadite as a sheet structure comprising units of $[M(TO_4)_2L_2]$ stoichiometry. However, this description only refers to the M = Nb (or Fe(2), in this case) octahedron and misses the significance of the Fe(1)O$_6$ chain; the three-dimensionality of the structure is probably a more useful description.

SUMMARY

We have prepared two new iron phosphates in hydrothermal systems involving addition of $C_2O_4^{2-}$ as a secondary anion. Both structures are related to known mineral structures and display structural features common in these systems. Unlike our recent report of a mixed anion framework structure in $Fe_4(PO_4)_2(C_2O_4)\cdot 2H_2O$ (10), the oxalate is not

incorporated into the phosphate structure in these reactions. Further work is ongoing to determine how widespread the cocrystallization of phosphate-organic anions in framework structures is likely to be, and results on new mixed anion frameworks will be reported in the near future.

REFERENCES

1. P. B. Moore, *Am. Mineral.* **55,** 135 (1970).
2. M. Cavellec, D. Riou, J.-M. Greneche, and G. Ferey, *Inorg. Chem.* **36,** 2187 (1997).
3. M. Cavellec, D. Riou, and G. Ferey, *J. Solid State Chem.* **112,** 441 (1994).
4. J. R. D. DeBord, W. M. Reiff, R. C. Haushalter, and J. Zubieta, *J. Solid State Chem.* **125,** 186 (1996).
5. K.-H. Lii and Y.-F. Huang, *Chem. Commun.* 839 (1997).
6. K.-H. Lii and Y.-F. Huang, *J. Chem. Soc., Dalton Trans.* 2221 (1997).
7. J. R. D. DeBord, W. M. Reiff, C. J. Warren, R. C. Haushalter, and J. Zubieta, *Chem. Mater.* **9,** 1994 (1997).
8. M. Cavellec, J. M. Greneche, D. Riou, and G. Ferey, *Microporous Mater.* **8,** 103 (1997).
9. M. Cavellec, D. Riou, C. Ninclaus, J. M. Greneche, and G. Ferey, *Zeolites* **17,** 250 (1996).
10. Z. A. D. Lethbridge and P. Lightfoot, JSSC, accepted.
11. P. T. Beurskens, G. Admiraal, G. Beurskens, W. P. Bosman, R. de Gelder, R. Israel, and J. M. M. Smits, "The DIRDIF-94 Program System," Technical Report of the Crystallography Laboratory. Univ. of Nijmegen, Netherlands, 1994.
12. teXsan Crystal Structure Analysis Package, Molecular Structure Corporation (1992).
13. I. D. Brown and D. Altermatt, *Acta Crystallogr. B* **41,** 244 (1985).
14. P. B. Moore, T. Araki, A. R. Kampf, and I. M. Steele, *Am. Mineral.* **61,** 5 (1976).
15. F. C. Hawthorne, *Acta Cystallogr. B* **50,** 481 (1994).
16. M. P. Attfield, R. E. Morris, I. Burshtein, C. F. Campana, and A. K. Cheetham, *J. Solid State Chem.* **118,** 412 (1995).